

Superconducting niobium nanowire single photon detectors

A. J. Annunziata,^a A. Frydman,^{a,c} M. O. Reese,^a L. Frunzio,^a M. Rooks,^b D. E. Prober^a

^aDepartment of Applied Physics, Yale University, 15 Prospect St. New Haven, CT, 06520-8284

^bIBM T. J. Watson Research Center, P.O. Box 218, Yorktown Heights, NY, 10598

^cDepartment of Physics, Bar Ilan University, Ramat Gan, Israel 52900

ABSTRACT

We have fabricated and tested single photon detectors based on a current biased superconducting niobium nanowire patterned into a meander. The detectors are fabricated from high quality, ultra high vacuum sputtered niobium thin films on a sapphire substrate. For detection of single optical photons, we show that the superconductor's intrinsic kinetic inductance does not limit the reset time of the detector, which is ≈ 2 nanoseconds, in contrast to the longer reset times seen in niobium nitride detectors of similar size and geometry. We also describe a readout scheme for photon counting that is unique to Nb due to its lower resistivity. These detectors have applications in imaging of infrared photoemission from CMOS logic circuits as well as in optical communications and quantum information processing.

Keywords: niobium, nanowire meander, superconducting single photon detector, reset time, kinetic inductance

1. INTRODUCTION

There are many applications at present and in the foreseeable future in which single photon detectors with low jitter, fast count rate, and sensitivity in the visible and infrared wavelengths are crucial. These varied applications include optical communication, quantum information processing, laser radar, and, in particular, CMOS process development using the technique of picosecond imaging circuit analysis developed at IBM.¹

Existing semiconductor-based technologies such as Si and InGaAs avalanche photodiodes (APDs) and photomultiplier tubes have too large a jitter (>100 ps), too slow a counting rate (<10 MHz), and other drawbacks such as afterpulsing (APDs) and high dark count rates that make them non-ideal for these applications. Other superconducting detectors such as superconducting tunnel junction detectors (Cooper pair-breaking charge sensors) or hot electron bolometers (superconducting transition edge thermal sensors) are either not sensitive enough for single photon detection or have too low a count rate or too slow a response.²

Recently, much work has gone into developing a new type of fast, single photon detector with extremely promising results. The detector consists of a current-biased superconducting niobium-nitride nanowire patterned into a meander to maximize the active area of the detector.^{3,4} These detectors have demonstrated as high as 75% internal quantum efficiency at 1550 nm with only tens of picoseconds of jitter and count rates of several hundred MHz.⁵

Although the count rate for small area NbN detectors is high, it is significantly lower for the most efficient detectors that have moderate to large area, e.g., $10 \times 10 \mu\text{m}^2$. (Initially, GHz counting rates were expected based on the extremely fast electron-phonon interaction time, and hence fast cooling, in NbN.⁶) In addition, there is currently no way to obtain spectral information or to distinguish a one photon event from a two photon event with a NbN detector, since absorbed radiation is recorded only as a "click" with the height of the resulting voltage pulse being essentially independent of the photon energy or number. Spectral resolution and photon number counting from the pulse amplitude would be extremely

useful in some applications. Finally, due to the difficulty of fabricating high quality, ultra-thin NbN films, only a few groups have mastered the film deposition process.⁷

Although NbN-based detectors have been the most extensively studied, this paper will show that there are a number of potential advantages for using Nb-based nanowire detectors. In particular, Nb is easier to work with, can offer a faster count rate for detectors of moderate to large ($100 \mu\text{m}^2$) area, and has the potential to yield a photon number resolving (or spectrally sensitive) detector. These advantages should make Nb an attractive material for SSPDs in certain applications.

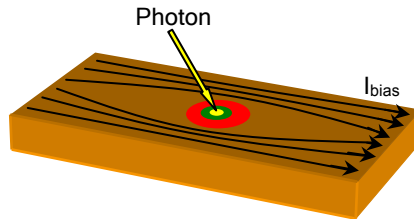


Fig 1: Detection mechanism.

2. DEVICE OPERATION

A superconducting nanowire single photon detector (SSPD) consists of a ~ 100 nm wide strip of superconducting material that is current biased near the critical current. When a photon is absorbed in the wire, it breaks a Cooper pair. After thermalization, a hotspot of quasiparticles is formed from which the supercurrent is expelled (Figure 1). Since the supercurrent is now squeezed into the “sidewalks” around the hotspot, the current density in these areas exceeds the critical value, and a normal region develops across the wire.⁴ Quasiparticle diffusion and Joule heating compete with various cooling mechanisms to determine the hotspot evolution in time.⁸ After some time, given by the details of this interplay between heating and cooling effects, the hotspot collapses and superconductivity is restored.

A simplified view of the readout circuit is seen in Figure 2. When an absorbed photon creates a transient resistive section in the detector element, a portion of the bias current is shunted to the amplifier and measured across the 50Ω input impedance of the microwave amplifier. A schematic of a typical voltage pulse that results from a detected photon is seen in Figure 3.

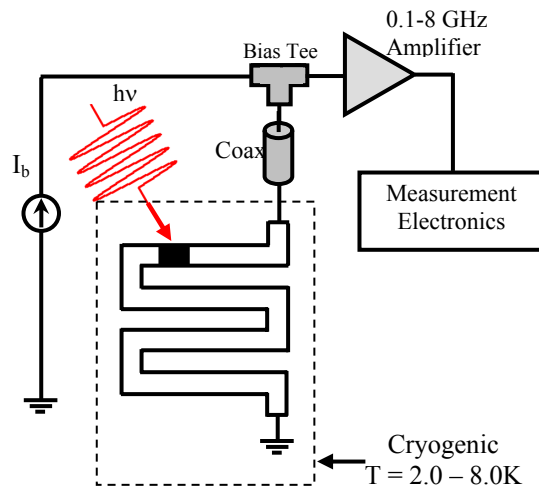


Fig. 2: The measurement circuit.

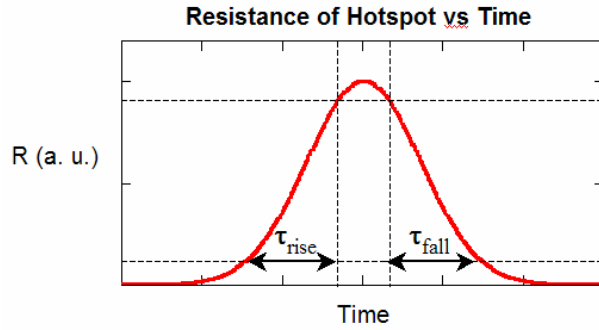


Fig. 3: Typical voltage pulse (schematic)

The important characteristics of the pulse are the rise time, the fall time, and the reset time. The rise time and fall time yield information about the underlying device physics. They are defined as the time it takes for the voltage pulse to grow from 10% to 90% and decay from 90% to 10% of its maximum value. The reset time is defined here to be the total time it takes the current in the device to return to 90% of its steady state value (value before the detection event) after the initial detection of a photon. Since the device needs to be biased near the critical current to have high detection efficiency, the reset time represents the time it takes for the device to recover a significant fraction of its detection efficiency.

The details of the signal, and in particular the peak height, depend on the normal state sheet resistance of the detector material. The voltage of the peak for the circuit of Figure 2 (with a 50Ω amplifier) is given by:

$$V = \frac{50 \cdot R_{HS}}{50 + R_{HS}} I_b \quad (1)$$

where R_{HS} is the resistance of the normal hot spot created due to the photon absorption. For NbN R_{HS} is approximately 1

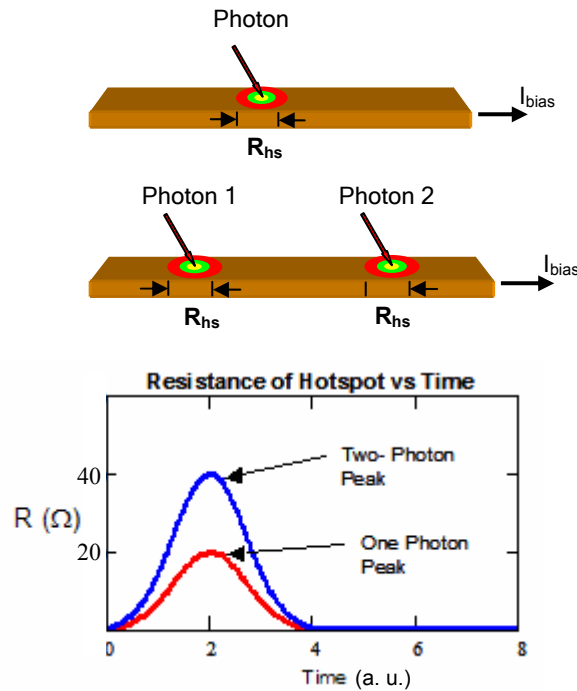


Fig. 4: Proposed photon counting scheme.

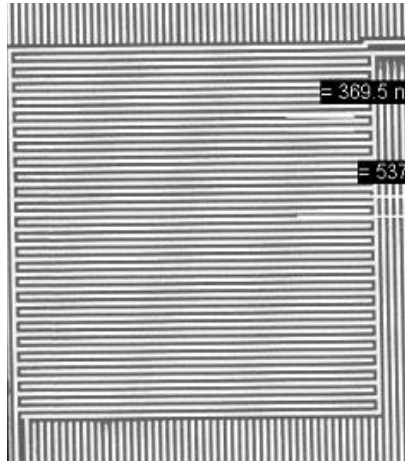


Fig.5: Electron micrograph of 100 nm wide nanowire meanders (Nb is dark). Parallel lines outside of meander are not connected.

$k\Omega$, much larger than the 50Ω input resistance of the amplifier. In this case, almost all of the bias current is shunted through the 50Ω amplifier during detection, and the measured voltage signal is just $I_b \times 50 \Omega$, where I_b is the dc bias current. Hence, for very large R_{HS} , as in the case of NbN, the peak height is relatively insensitive to the actual resistance, and thus independent of hotspot size. For our Nb nanowires, R_{HS} is of order 20Ω , and thus the amplitude of the voltage pulse should depend significantly on the hotspot resistance. The hotspot size is expected to depend on the photon energy; this should be apparent for a Nb based detector with a 50Ω amplifier, but not for a NbN detector. Further, a simple photon-counting scheme based on low-resistance Nb nanowires is seen in Figure 4. Since the detector consists of a long wire, if two photons are absorbed at once, the hotspots are unlikely to overlap, leading to two independent resistive sections of the wire and therefore twice the total series resistance. In Nb, this should be read out as a significantly larger amplitude voltage pulse, since for a higher device resistance, more current would be shunted to the 50Ω amplifier. NbN detectors display almost no such sensitivity to photon number.

Recent measurements on NbN detectors have uncovered another issue: an intrinsic tradeoff between reset time and detection area in these detectors.⁵ This is due to the high kinetic inductance, L_k , of NbN films. For a superconducting wire, the kinetic inductance scales with its length. For the nanowire meander detectors studied, the length scales with the detection area.

A large kinetic inductance slows down the detector performance, since the fall time is then determined by L_k/R where R is the 50Ω input resistance of the amplifier. This means that for a NbN detector with a reasonable area, the photon counting rate will be limited by L_k . Indeed, recent work shows that although fall times were faster than 1 ns for short ($5 \mu\text{m}$) NbN wires⁵, for $500 \mu\text{m}$ long meanders, the fall times were ~ 10 ns, thus limiting the reset frequency to approximately 100 MHz, lower than the desired count rate. The long meander was in a $10 \times 10 \mu\text{m}^2$ detector.

The situation is expected to be different for Nb. For a narrow superconducting wire,

$$L_k \propto \lambda^2 \cdot \mu_0 \cdot \frac{l}{A} \quad (2)$$

where l is the length of the wire, A is the wire cross sectional area, λ is the penetration depth, and μ_0 is the vacuum magnetic permeability.⁹ The penetration depth of Nb is approximately 5 times smaller than for NbN, therefore the kinetic inductance is approximately a factor of 25 less than in NbN for the same geometry wire.¹⁰ This means that Nb detectors have the potential for high count rates even for large detector areas, to over $100 \mu\text{m}^2$.

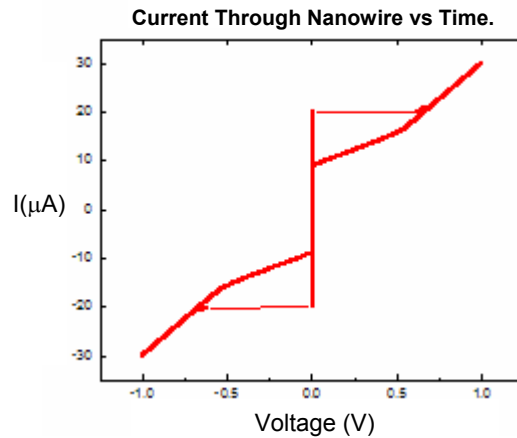


Figure 6: DC IV curve for 200nm wide nanowire detector showing a critical current of approx. 20 μA .

3. SAMPLE FABRICATION

The SSPDs tested in this work consisted of long wires (250-500 μm) patterned into a meander, which maximizes the detection area. The meanders consisted of 100 and 200 nm lines with a 50% fill factor patterned from 10 nm thick films (Figure 5). The detectors were fabricated using electron beam lithography. The Nb thin films were deposited using dc sputtering in an ultra high vacuum (base pressure: 3×10^{-9} torr) Kurt J. Lesker sputtering system on 2-inch R-plane sapphire substrates at room temperature. The Nb was patterned using electron beam lithography and reactive ion etching. Typical 10 nm thick Nb wires on sapphire have a transition temperature, T_c , of 5.5 K. A typical dc IV curve at $T = 4.2$ K is shown in Figure 6, in this case for a 200 nm wide strip with a critical current of approximately 20 μA .

4. MEASUREMENT SETUP

The cryogenic measurement system allows precise temperature control, excitation using fiber-coupled ultraviolet photons, and low noise dc and high frequency electrical measurements. Samples were cooled to between 2.0 K and 4.2 K in a pumped ^4He cryostat utilizing a vacuum isolated stage for precise thermal control. Temperature was controlled using a resistive heater and measured using a RuO_4 thermometer.

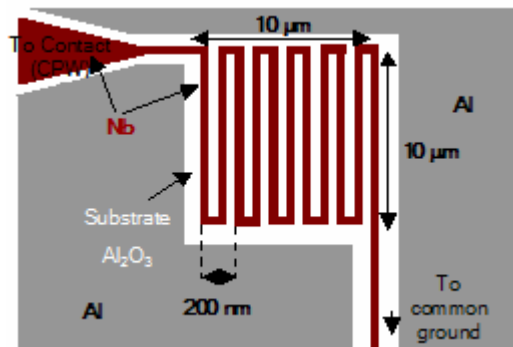


Fig. 7: Chip layout. The dimensions of the nanowire meander are not drawn to scale.

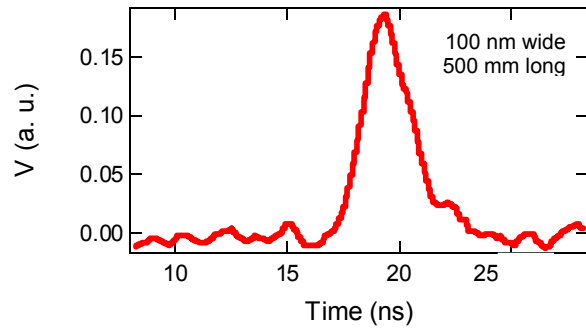
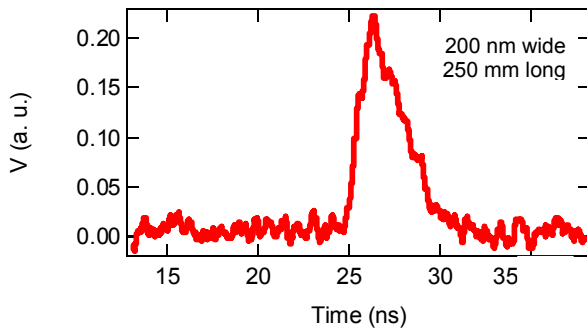
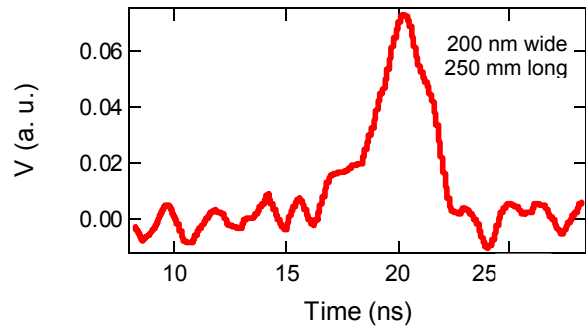
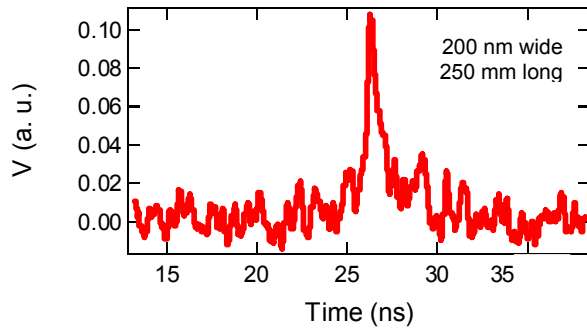


Figure 8: Voltage pulses from a $10 \times 10 \mu\text{m}^2$ meander for different levels of laser attenuation. The relatively noisy data results from using an early preamplifier with relatively large input noise. The longer pulse is due to the delay between multiple photons arriving during the long laser pulse, as explained in the text. The shorter pulse (upper) indicates the speed of the combined detector and electronics.

Figure 9: Upper: voltage pulse for 200 nm-wide wire meander; lower: voltage pulse for 100 nm-wide wire meander; area = $10 \times 10 \mu\text{m}^2$

High frequency signals are coupled out of the detector using an on-chip thin-film coplanar waveguide (CPW) (Figure 7) that is wire-bonded to a CPW patterned on printed circuit board with the same dielectric constant as sapphire. A 4-channel cryogenic dc-18 GHz RF switch was utilized, which enables the testing of as many as 4 devices in the same cool down. Because of packaging issues, the switch is located beneath the sample mounting stage, necessitating a novel, right-angle through-substrate CPW-to-coaxial transition, which has been designed with reactive compensation of stray capacitances and inductances associated with the impedance discontinuity at the transition in order to minimize reflection.

The detectors were illuminated with 337 nm photons coupled from a multimode fiber positioned approximately 1 mm above the devices. The source of 337 nm light was an LSI pulsed N_2 laser with an approximately 4 ns (FWHM) pulse and 30 Hz repetition rate. Laser pulses are attenuated using a series of neutral density filters and coupled to the sample using a multimode fiber. In addition to dc and high frequency testing of each device, a large area film was patterned on every chip in order to test properties of the Nb films near each set of 4 devices under test, which may vary from chip to chip due to processing variations.

High frequency signals (> 10 MHz) and dc biasing are split using a bias tee (Mini Circuits, model ZFBT-4R2GW adapted for cryogenic use). DC biasing is provided by a resistor (typically $100 \text{ k}\Omega - 10 \text{ M}\Omega$) in series with a low noise voltage source (Yokogawa model 7651 or in some cases home-built bias electronics). Low frequency measurements are made using a Stanford model SR830 lock-in amplifier and Lab View. High frequency signals undergo two stages of amplification; the first stage is a Miteq AFS3-00100800 ultra low noise cryogenic amplifier, with a $0.1 - 8$ GHz

bandwidth. The second stage amplifier is a Miteq AFS5-00100800 low noise amplifier, with a 0.1 – 8 GHz bandwidth. Measurement is made using an Agilent model 54855A oscilloscope with a 6 GHz single-shot bandwidth and Lab View.

5. RESULTS

Measurements are reported for several 100 nm and 200 nm wide nanowire meanders. Figure 8 shows two pulses, with different amplitudes, from the same detector with different intensities of incident laser power. This pulse height difference was seen in all devices tested and scaled with the laser power. This amplitude difference indicates a sensitivity to the hot spot resistance. Specifically, when multiple photons are absorbed, a larger total normal resistance results from the multiple hotspot resistances adding in series. No similar behavior has been reported for NbN detectors. Note that the longer duration of the larger pulses (approximately 3 ns rise and 2 ns fall) is an artifact of the exciting laser's relatively long pulse (4 ns), which yields photons that do not overlap perfectly in time.

In Figure 9, pulses from detectors with two different lengths are shown. Figure 9 (top) shows a typical pulse from a 200 nm wide wire in a $10 \times 10 \mu\text{m}^2$ meander. Figure 9 (lower) shows a typical pulse for a 100 nm wide wire in a $10 \times 10 \mu\text{m}^2$ meander. The difference in kinetic inductance for these two is a factor of 4 ($l/A = \text{nanowire length/linewidth}$), yet there is no discernable difference in the fall time. In addition, for each of these long nanowires, reset times as fast as 2 ns have been seen, yielding count rates possibly as high as 500 MHz. This is faster than the larger area NbN detectors. The fastest pulses are characterized by the data in Figure 8 (upper). This indicates the speed of the combined detector and electronics. The pulses shown in Figure 9 and in Figure 8 (lower) are longer than the pulse seen in Figure 8 (upper) because they represent events where several photons are absorbed and hence their width in time is determined largely by the pulse length of the laser. They were chosen because the signal-to-noise ratio is high and demonstrate clearly that the rise and fall times are the same even for different length nanowires.

6. CONCLUSION/FUTURE WORK

In this preliminary study of Nb nanowire single photon detectors, two important results have been demonstrated. First, it has been shown that kinetic inductance is not a large factor in the reset time of the detectors. Because of this, high count rates are possible even from large area meander detectors that are likely to have high detection efficiency. Even faster count rates appear feasible with better quality Nb films. Second, the concept of photon number resolution from the signal amplitude (or spectral resolution of single photons) has been suggested, and data has been shown that suggests this is possible.

This has been only a preliminary study and proof of concept. Although current results are promising, much work remains. Future plans include precise measurements of quantum efficiency, jitter, photon counting with visible as well as infrared photons, optimization of the Nb films for higher T_c and faster cooling, and a deeper study of the underlying physics of the hotspot dynamics.

REFERENCES

- ¹ J. C. Tsang, et al. "Picosecond imaging circuit analysis," IBM Journal of Research and Development **44**, No. 4, pp. 583-604 (2000).
- ² Applied Superconductivity Conference (2004). See IEEE Trans Appl. Supercond. **15** (2005).
- ³ K. S. Il'in, et al. "Pico-second hot-electron energy relaxation in NbN superconducting photo-detectors," Appl. Phys. Lett. **76**, pp. 2752-2754 (2000).
- ⁴ A. Semenov, et al. "Quantum detection by current carrying superconducting film," Physica C **352** pp. 349-356 (2001).
- ⁵ A. J. Kerman, et al. "Kinetic inductance limited reset time of superconducting nanowire photon counters," Appl. Phys. Lett. **88**, 111116 (2006).
- ⁶ A. Pearlman, et al. "Gigahertz counting rates of NbN single-photon detectors for quantum communications," IEEE Trans. Appl. Supercond. **15**, No. 2, pp. 579-582 (2005).

⁷ Gol'tsman, et al. "Response time characterization of NbN superconducting single-photon detectors," IEEE Trans. Appl. Supercond. **13**, No. 2, pp. 180-183 (2003).

⁸ J. K. W. Yang, et al. IEEE Trans. Appl. Supercond. (2007), to appear.

⁹ T. Van Duzer and C. W. Turner. *Superconductive Devices and Circuits*, Prentice Hall (1999).

¹⁰ We use values of H_{C2} and/or resistivity to infer the Ginzberg-Landau coherence length and thereby compute λ . See M. Tinkham, *Introduction to Superconductivity*, Dover Publications (1996). NbN data from D. W. Deis, et al. "High field properties of pure niobium nitride thin films," J. Appl. Phys. **40**, pp. 2153-2156 (1969). Nb data from M. O. Reese, Ph.D. Thesis, Yale University, 2006 (unpublished).